

Period – magnitude relationships in *BVIJHK*-bands for fundamental mode and first overtone Cepheids

I. Baraffe^{1,2} and Y. Alibert¹

¹ C.R.A.L (UMR 5574 CNRS), École Normale Supérieure, 69364 Lyon Cedex 07, France

² Max-Planck-Institut für Astrophysik, Karl-Schwarzschildstr.1, 85748 Garching, Germany
e-mail: yalibert@ens-lyon.fr

Received 9 November 2000 / Accepted 8 March 2001

Abstract. We present theoretical period – magnitude relationships for Cepheids in different filters for fundamental and first overtone pulsators, completing the work by Alibert et al. (1999). The results are provided for different metallicities characteristic of the Magellanic Clouds and the Milky Way. In contrast to the fundamental mode, we find a small metallicity effect on the period – luminosity relationship for the first overtone, due to the sensitivity of the period ratio P_1/P_0 with metallicity. Comparison is made with observations from OGLE and EROS in the Small and Large Magellanic Clouds. We emphasize the constraint on theoretical predictions provided by the combination of both fundamental and first overtone observed sequences. We obtain excellent agreement between models and data in a $\log P - W_I$ (Wesenheit index) diagram for a distance modulus for the LMC $\mu_0 = 18.60 - 18.70$. We analyse the uncertainties of the fundamental period – magnitude relationships and the consequences on distance determination. We show that an arbitrary shift of the instability strip by 350 K in T_{eff} yields up to 0.45 mag effect on M_V at a given period, whereas the effect is less than 0.1 mag in the K -band. Using recent near-IR observations in the Large Magellanic Cloud and our $P - M_K$ relationship, we derive a distance modulus for the LMC in agreement with the value based on W_I data.

Key words. stars: evolution – stars: distances – Magellanic clouds – distance and redshift

1. Introduction

Over the last five years, a wealth of data for Cepheids was collected by several observational projects (HST key project, HIPPARCOS, microlensing experiments EROS, MACHO, OGLE, etc.). This fantastic amount of data allows unprecedented opportunities to understand the properties of these variable stars. One of the relevance of Cepheids, and the main goal of the HST key project (cf. Freedman 2000, and references therein), is the determination of local extragalactic distance scales and consequently of the Hubble constant H_0 . The period – luminosity relationship (PL) of Cepheids is the cornerstone of such an analysis purpose. An important contribution to the collection of data is provided by microlensing search projects toward the Magellanic Clouds (EROS: Renault et al. 1996; OGLE: Udalski et al. 1997; MACHO: Alcock et al. 1997; and references therein). The recent release into the public domain of their Cepheid Catalog (EROS: Afonso et al. 2000; OGLE: Udalski et al. 1999a,b) provides large, homogeneous samples of high quality data which in principle

allow a deep analysis of the period-luminosity relationships. In particular, a key question related to the PL relationship is its dependence on metallicity. This is of fundamental importance for extragalactic distance scales, usually based on an universal PL relationship. A controversy still exists regarding metallicity effects, both from an observational and theoretical viewpoint (see Alibert et al. 1999 and references therein). Another notorious debate concerns the distance to the LMC, which is an important source of uncertainty in the determination of H_0 (see Freedman 2000). Although PL relationships used for distance estimate are based on fundamental (F) pulsators, the afore-mentioned catalogs also provide statistically significant samples of first overtone (1H) Cepheids. Because of the distinction of F and 1H pulsator sequences in period – magnitude diagrams, 1H provides additional constraints on theoretical models and on distance determinations based on PL relationships.

In a recent paper, Alibert et al. (1999) performed self-consistent stellar evolution and linear stability analysis calculations for Cepheids. Their analysis was essentially devoted to fundamental mode pulsators and their period-magnitude-color relationships as a function of metallicity.

Send offprint requests to: I. Baraffe,
e-mail: ibaraffe@ens-lyon.fr

The analysis of their results for first overtone pulsators and the comparison with observations was hampered at that time by the lack of significant samples of data. The aim of the present paper is to complete the work of Alibert et al. (1999) for first overtone pulsators and test their results against the observational constraints provided by *both* F and 1H pulsators. In Sect. 2, we derive PL relationships for 1H and in Sect. 3 we compare the results to observations. In Sect. 4, we briefly discuss the uncertainties of our period – magnitude relationships and consequences on distance determinations.

2. Period – magnitude relationships for first overtone pulsators

The description of the stellar evolution and pulsation calculations are given in details in Alibert et al. (1999). We recall the main ingredients: (i) evolutionary models for Cepheids are constructed with the Lyon evolutionary code from 3 to 12 M_{\odot} . We consider various initial compositions $(Z, Y) = (0.02, 0.28)$, $(0.01, 0.25)$ and $(0.004, 0.25)$ ¹, representative of respectively the Galactic, the Large Magellanic (LMC) and the Small Magellanic (SMC) clouds environments. Evolutionary calculations do not include core overshooting. (ii) A linear non-adiabatic stability analysis is performed on the complete evolutionary models along the evolutionary tracks. This provides consistent mass-age-period-luminosity relations. (iii) Static atmosphere models and their corresponding synthetic spectra are calculated for the same compositions used in (i), providing magnitudes and colors for a given $(Z, M, L, T_{\text{eff}})$.

2.1. Period – luminosity and period – magnitude relationships in different filters

In order to derive statistical PL relationships, a mean position is assigned to each mass, according to the time spent in different locations in the instability strip (IS) and a linear least-square fit to these points is derived. As shown in Alibert et al. (1999), the mean position of a given stellar mass, accounting for its evolutionary time, is roughly located in the middle of the IS.

The minimum masses m_{min} undergoing a blue loop in the 1H instability strip are 3.25 M_{\odot} , 4 M_{\odot} and 5 M_{\odot} for respectively $Z = 0.004$, 0.01 and 0.02. In order to avoid biases due to the change of slope predicted near these minimum masses (see Alibert et al. 1999, their Sect. 3.4), we exclude in the present analysis m_{min} to derive the mean PL relationships. Because of the reduction of the blue loop extension toward lower masses, the slope of the PL relationships for 1H can be affected if the fit is derived down to m_{min} , yielding steeper relations. Bauer et al. (1999) observed such a change of slope for fundamental pulsators in the SMC, but did not observe it for 1H, although predicted

Table 1. Coefficients of the $\log P$ (in days) – $\log L/L_{\odot}$ relationships (slope, zero-point) for first overtone pulsators as a function of metallicity

$Z = 0.02$	(1.247, 2.659)
$Z = 0.01$	(1.252, 2.646)
$Z = 0.004$	(1.257, 2.613)

by the models (see the discussion by Alibert et al. 1999, Sect. 4.2.3). The relationships given in Tables 1 and 2 are then derived from 3.5 M_{\odot} for $Z = 0.004$, 4.25 M_{\odot} for $Z = 0.01$ and 5.5 M_{\odot} for $Z = 0.02$. Note that Alibert et al. (1999) derived preliminary PL relationships for 1H based on the whole range of masses unstable in the IS (including m_{min}) and obtained slightly different results than in Table 1.

The period – magnitude relationships in different filters are given in Table 2 for F and 1H modes. *BVRI* magnitudes are based on the Johnson-Cousins system (Bessell 1990) and *JHK* magnitudes are defined in the CIT system (Leggett 1992). Table 2 displays also the reddening-free Wesenheit index $W_I = I - 1.55(V - I)$ (Madore & Freedman 1991), with the coefficient 1.55 ($= A_I/E(V - I)$) resulting from standard interstellar extinction curves (e.g., Schlegel et al. 1998).

2.2. Effects of metallicity

Figure 1 displays the mean $\log P_1 - \log L/L_{\odot}$ relationships (Fig. 1a) and the blue and red edges in a $\log P_1 - T_{\text{eff}}$ diagram (Fig. 1b) as a function of Z . Excluding the minimum mass undergoing a blue loop in the IS, which decreases with Z , there is no noticeable effect of Z on the location and width of the IS in Fig. 1b. The periods corresponding to m_{min} in Fig. 1 are $\log P_1 \sim 0.3, 0.1$ and 0 for respectively $Z = 0.02, 0.01$ and 0.004. We note however a small effect of Z on the PL relationship, with $\log L$ increasing by 0.04 for Z increasing from 0.004 to 0.02 at a given P_1 .

In the following, our analysis is restricted to period $\log P_1 \geq 0.3$, since $\log P_1 = 0.3$ is the minimum period for $Z = 0.02$ 1H pulsators undergoing a blue loop (see Fig. 1). An inspection of the relationships given in Table 1 shows that the slopes hardly depend on Z , but the zero points are affected by metallicity. Although small, the increase of L with Z translates in brighter magnitudes at a given P_1 , with the largest effects in the *VIJ* bands and the maximum effect in the *I* band. We note that M_V, M_I and M_J are brighter by 0.1 – 0.15 mag, M_H and M_K are brighter by 0.8 – 0.13 mag at a given P_1 when Z increases from 0.004 to 0.02. Between $Z = 0.004$ and $Z = 0.01$ the effect is ~ 0.1 mag in the *VIJHK* bands. Interestingly enough, the effect is the smallest in the *B* band, with a difference of M_B less than 0.1 mag between $Z = 0.004$ and $Z = 0.02$. Opposite trends are found for fundamental mode PL relationships which show the largest Z effect in

¹ Z is the metal mass fraction and Y the helium mass fraction.

Table 2. Coefficients of the log P (in days) – magnitude relationships (slope, zero-point) for fundamental mode (upper row) and first overtone (lower row) as a function of metallicity

Z	M_B	M_V	M_I	M_J	M_H	M_K	W_I
0.02	(-2.658, -0.648) (-2.669, -1.561)	(-2.905, -1.183) (-2.948, -1.990)	(-3.102, -1.805) (-3.171, -2.526)	(-3.256, -2.183) (-3.333, -2.844)	(-3.346, -2.428) (-3.434, -3.042)	(-3.367, -2.445) (-3.453, -3.057)	(-3.407, -2.770) (-3.515, -3.355)
0.01	(-2.712, -0.655) (-2.699, -1.515)	(-2.951, -1.153) (-2.972, -1.923)	(-3.140, -1.769) (-3.192, -2.463)	(-3.286, -2.157) (-3.356, -2.795)	(-3.377, -2.411) (-3.461, -3.006)	(-3.395, -2.428) (-3.481, -3.019)	(-3.433, -2.725) (-3.534, -3.300)
0.004	(-2.707, -0.633) (-2.765, -1.430)	(-2.939, -1.081) (-3.01, -1.807)	(-3.124, -1.686) (-3.212, -2.341)	(-3.262, -2.076) (-3.376, -2.678)	(-3.351, -2.336) (-3.478, -2.898)	(-3.369, -2.350) (-3.501, -2.906)	(-3.411, -2.623) (-3.545, -3.170)

the B band, but small effects (less than 0.1 mag) at longer wavelengths (see Alibert et al. 1999, Sect. 5).

This effect of Z on the PL relationship for 1H is related to the behavior of the period ratio P_1/P_0 as a function of Z . This ratio decreases as Z increases (cf. Baraffe et al. 1998): we find for $Z = 0.004$, $P_1/P_0 \sim 0.73$ and for $Z = 0.02$, $P_1/P_0 \sim 0.7$. Since for a given L , P_0 is essentially independent of Z , P_1 decreases because of decreasing P_1/P_0 ratio for increasing Z . Conversely, for a given P_1 , L increases with Z .

The behavior of P_1/P_0 with Z can be understood by analysing the regions in the star which contribute to the period of each mode. Such regions can be determined by the Epstein weight functions which are obtained by expressing the eigen frequency of each mode by an integral over the whole star (Epstein 1950; Cox 1980). As already noted by Epstein (1950), the greatest contribution to the fundamental mode period is located between $r/R \sim 0.7$ and $r/R \sim 0.9$. For the first overtone, two regions are important: a first inner region located between $r/R \sim 0.4$ and $r/R \sim 0.7$ and an outer zone with $r/R > 0.85$. These regions are characteristic of the mass range of interest (5–10 M_\odot). The inner region for 1H includes the opacity peak due to metals at $T \sim 2 \cdot 10^5$ K and the outer region covers the H-He ionization zone. In the first region covering the metal opacity peak, an increase of the opacity κ , related to an increase of the metallicity, yields an increase of T or a decrease of the density ρ at fixed r (or P). Note that this region is dominantly radiative and the temperature gradient depends directly on Z since the radiative gradient is proportional to κ . Consequently, in this region, the sound speed $C_s \propto (P/\rho)^{1/2} \propto T^{1/2}$ is more sensitive to the metallicity than in other outer regions and increases with Z . The integral of the sound travel time $\tau_s = dr/C_s$ through this zone is thus more sensitive to the metallicity, decreasing as Z increases, than in the other regions located at $r/R > 0.7$. The period ratio P_1/P_0 is related to the ratio of τ_s through the regions relevant for 1H to τ_s in the zones contributing to F. Because of the larger sensitivity to Z of τ_s for 1H, this ratio decreases as Z increases. We checked our arguments by calculating the integral of τ_s through the different regions of interest for different cases of M , L and T_{eff} covering the instability strip and for different values of Z .

The behavior of L as a function of P_1 with Z explains the trends previously mentioned of the fluxes in different filters. In particular, it explains the low sensitivity of the log $P_1 - M_B$ relationship to Z because of the

compensating effects of (i) higher L with increasing Z at a given P_1 and (ii) lower B -flux for a given L and T_{eff} as Z increases, because of more metallic line absorption in the B bandpass (see Sect. 5 of Alibert et al. 1999).

Finally, because of the maximum effect in the I -bandpass, we note a non negligible effect of Z on the index W_I , which differs by 0.14 mag at long P_1 up to 0.18 mag at shorter P_1 between $Z = 0.004$ and 0.02. When Z increases from 0.004 to 0.01, W_I gets brighter by ~ 0.13 mag.

3. Period – magnitude diagrams: Comparison with observations

Comparison with observations are made with the EROS2 and OGLE2 data for the MC. EROS2 (Afonso et al. 2000) reports 239 1H Cepheids in the SMC and 113 in the LMC. OGLE2 provides ~ 800 1H pulsators in the SMC and ~ 500 in the LMC.

3.1. SMC Cepheids: VI-bands

Figure 2 displays the comparison between models with metallicity $Z = 0.004$ and the OGLE2 data. EROS2 data are not shown for the sake of clarity, but are comparable to the OGLE2 data. We adopt the dereddened data provided by the OGLE2 catalog, with different reddening corrections for each fields (see Udalski et al. 1999b for details) and the same distance modulus $\mu_0 = 18.94$ as used in Alibert et al. (1999). This value, suggested by Laney & Stobie (1994), yields general agreement between models and various observations for fundamental pulsators (cf. Alibert et al. 1999). Unstable models during the first crossing phase (large open circles) and the core He burning blue loop (filled circles) are indicated (see Alibert et al. 1999 for details). As shown in Fig. 2, a general good agreement is found for 1H pulsators. The fundamental mode sequence is indicated by the mean PL relationship, and compared to the relationship of Udalski et al. (1999c), recently revised by Udalski (2000). Note that these authors truncate their SMC sample at $\log P < 0.4$, to avoid biases at short periods. The agreement between predicted and observed F relationships is thus excellent for $\log P > 0.4$. As preliminary noted by Alibert et al. (1999) and confirmed by the data, observations for 1H do not extend above $\log P \sim 0.6$, which corresponds to $m \sim 5 M_\odot$ with standard (no overshooting) evolutionary models. Note that models including overshooting would yield a lower mass for such period. Our linear stability

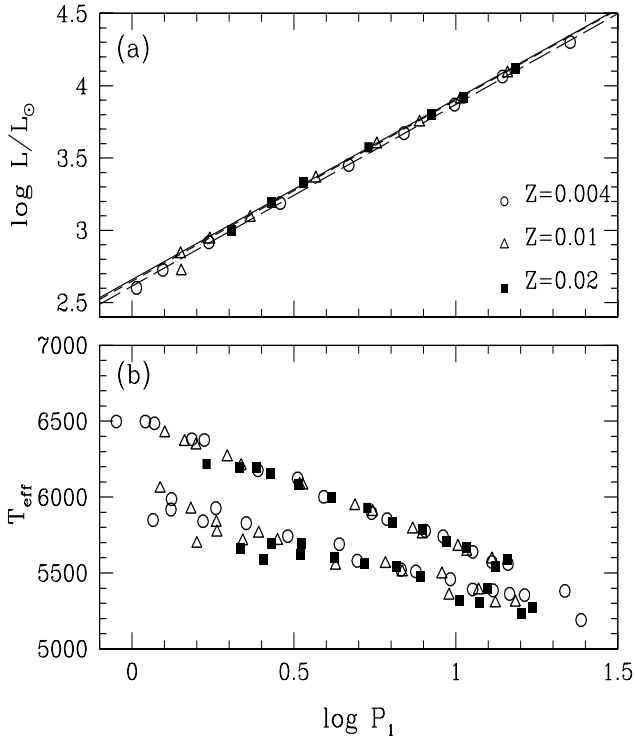


Fig. 1. **a)** $\log P$ (in days) – L diagram for 1H pulsators and different metallicities. The symbols indicate the mean position of each mass in the IS as a function of Z . The mean PL relationships are plotted for $Z = 0.02$ (solid line), $Z = 0.01$ (dashed line) and $Z = 0.004$ (long dashed-line). **b)** Location of the blue and red edges of the 1H IS in a $\log P - T_{\text{eff}}$ diagram. The symbols correspond to the same Z as in **a)**. The minimum masses undergoing a blue loop in the IS are $3.25 M_{\odot}$, $4 M_{\odot}$ and $5 M_{\odot}$ for respectively $Z = 0.004$, 0.01 and 0.02

analysis however finds unstable 1H modes (as well as F modes) for masses $m > 5 M_{\odot}$. Only non-linear calculations can determine the dominant mode of pulsation. In the same vein, models predict that 1H pulsators with $\log P \lesssim 0$ are in the first crossing phase. The significant number of such low period pulsators provides another strong constraint on non-linear calculations which could test the following scenarios: (1) models on the first crossing, characterised by a lower luminosity than during the He core burning blue loop for a given mass, should favor 1H as the dominant mode, and (2) models with $m \gtrsim 5 M_{\odot}$ on the blue loop should oscillate predominantly in the fundamental mode.

We note however that in case (1), one may expect a change in the number density of objects with $\log P \lesssim 0$, given the much faster evolutionary timescale on the first crossing compared to the blue loop phase. Such a change is not displayed by current observations. A detailed statistical analysis taking into account evolutionary timescales, mass functions and eventual observational biases is required to investigate this point.

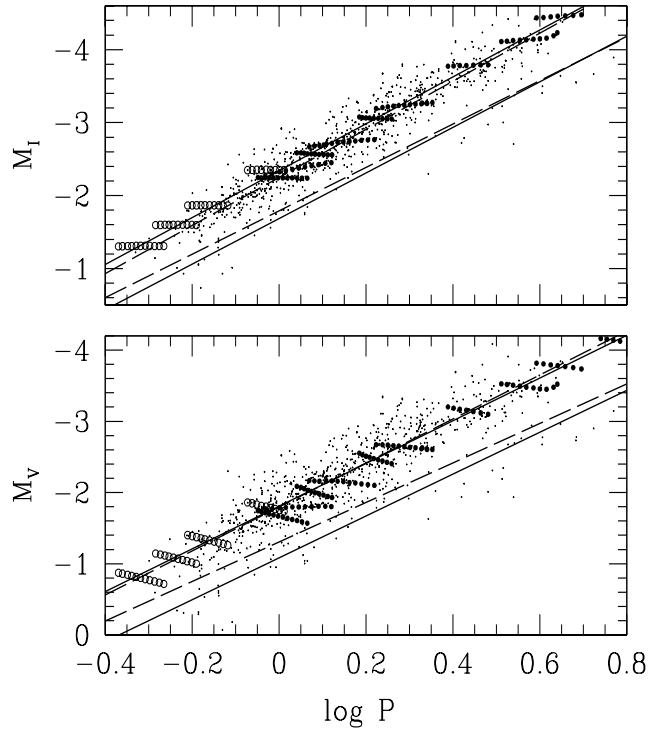


Fig. 2. Period (in days) – magnitude diagrams for 1H pulsators in the VI bands for models with $Z = 0.004$ and SMC observed Cepheids. The filled circles correspond to unstable 1H modes during core He burning phase from $m_{\text{min}} = 3.25 M_{\odot}$ to $6 M_{\odot}$. The large open circles correspond to first crossing unstable 1H modes for 3, 3.25, 3.5 and $4 M_{\odot}$. Observations (dots) are from OGLE2 (Udalski et al. 1999b). The distance modulus is 18.94. The 2 solid curves are the theoretical mean PL relationships for respectively F (lower curve) and 1H (upper curve) pulsators. The long-dashed curves are the observed PL relationship derived by Udalski et al. (1999c) and Udalski (2000) for F and 1H pulsators

3.2. LMC Cepheids: VI -bands

Comparison between models with $Z = 0.01$ and observations in the LMC is shown in Fig. 3. Data are from EROS2 (Afonso et al. 2000) and OGLE2 (Udalski et al. 1999a). We adopt the same reddening correction as in Udalski et al. (1999a) for the OGLE2 sample, which varies from field to field. For the EROS2 data, we adopt the same reddening correction $E(B - V) = 0.10$ as used in Alibert et al. (1999). We note that adopting a constant $E(B - V) = 0.10$ for the OGLE2 data has no noticeable effect when comparing models and data in Fig. 3. We adopt the same distance modulus 18.50 as in Alibert et al. (1999). The theoretical PL relations for F and 1H modes are compared to the observed relations derived by Udalski et al. (1999c) on the LMC sample limited to $\log P > 0.4$, and recently revised by Udalski (2000). The same agreement as for the SMC data is found and the models reproduce the width and location of the instability strip satisfactorily. We however note discrepancies between models and observations for the *mean* $P - M_V$ relationship for both F and 1H modes. This discrepancy appears also, but to a lesser extent, for

the SMC (cf. Fig. 2) and is better illustrated in $P - W_I$ diagrams (see next section).

As illustrated in Fig. 3, no 1H pulsators are observed above $\log P \sim 0.8$, corresponding to $m \gtrsim 7 M_\odot$. Note that the lack of 1H pulsators at long periods could also be interpreted in terms of very small amplitudes below the level of detection of OGLE or EROS. However, there is no obvious decrease of the amplitudes of 1H pulsators in the LMC, as well as in the SMC (see Afonso et al. 1999), as the period increases which could support this interpretation. Below $\log P \sim 0.1$, observations can be explained by first crossing models. We therefore find the same type of constraints as derived in the previous section for the determination of the dominant pulsating mode. Such comparisons suggest that the afore-mentioned properties in scenarios (1) and (2) (see Sect. 3.1) are intrinsic to 1H pulsators for Z varying from 0.004 to 0.01. More observations at higher metallicities are currently required to determine if these properties apply also to Galactic Cepheids.

3.3. $P - W_I$ diagram

Figures 4 and 5 display observations and models for both F and 1H in a $\log P - W_I$ diagram, for respectively the SMC and the LMC. The Wesenheit index W_I is an useful quantity since it is rather insensitive to the reddening and can in principle remove part of the scatter due to differential reddening. For the LMC, the $Z = 0.01$ models are also compared to observations from Gieren et al. (1998) for F Cepheids. Note that Alibert et al. (1999) found good agreement in different optical and near-infrared $P -$ magnitude diagrams with the latter sample of data. As expected, the scatter of data in such diagram is smaller than in the V and I bands. A first inspection of Figs. 4 and 5 show a general agreement between models and observations for both SMC and LMC: the models corresponding to different masses cover the observed location of both F and 1H Cepheids. We note that the models are in better agreement with the observed width of the IS in the LMC, whereas the data in the SMC show a larger scatter. This is consistent with the recent analysis by Groenewegen (2000) who interprets the larger dispersion in the PL relation in W_I for the SMC compared to the LMC in terms of a larger intrinsic depth of the former Cloud.

For both the SMC and the LMC, the predicted $\log P - W_I$ mean relationships are shifted compared to the observed relationships. Since the shift between observed and predicted relationships is *almost constant* on the whole range of P and is the *same* between F and 1H relations, we find that an increase of the distance moduli μ_0 by the same amount $\sim 0.15 - 0.2$ mag for both clouds removes easily this discrepancy. This is illustrated in the insets of Figs. 4 and 5. Note that such an increase of μ_0 does not alter the agreement found between observations and models in the I -band (see Figs. 2 and 3). It however increases the discrepancy in the V -band mentioned in the previous

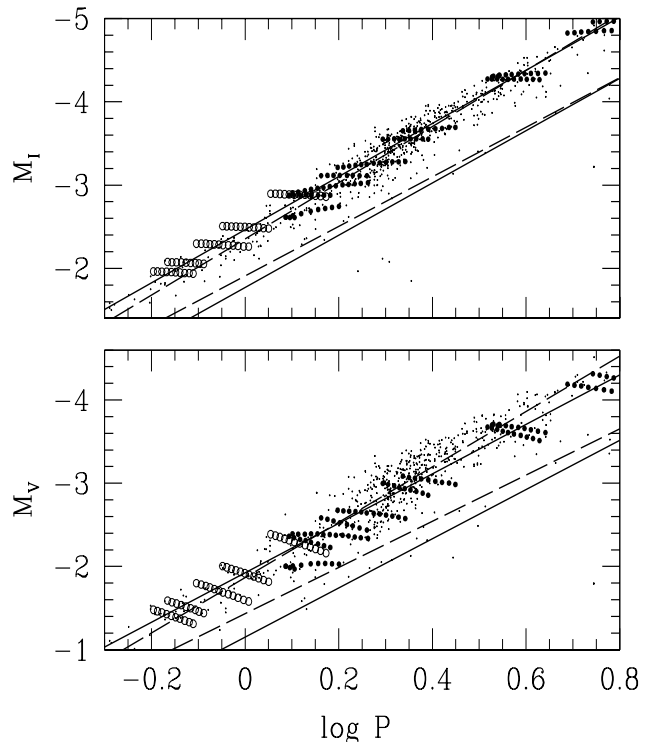


Fig. 3. Period (in days) – magnitude diagrams for 1H pulsators in the VI bands for models with $Z = 0.01$ and LMC observed Cepheids. The filled circles correspond to unstable 1H modes during core He burning phase from $m_{\min} = 4 M_\odot$ to $7 M_\odot$. The open circles correspond to first crossing unstable 1H modes for 3.875, 4, 4.25, 4.5, $5 M_\odot$. Observations (dots) are from OGLE2 (Udalski et al. 1999a) and EROS2 (Afonso et al. 2000). The distance modulus is 18.50. The 2 solid curves are the theoretical mean PL relationships for respectively F (lower curve) and 1H (upper curve). The 2 long-dashed curves are the observed PL relationships derived by Udalski et al. (1999c) and Udalski (2000)

section. It is difficult to analyse the reason for such inconsistency. The choice of the reddening and of the extinction curve coefficients, affecting mostly the V -band, could be the reason. This emphasizes the large uncertainties intrinsic to observations in this filter and suggests rather to use W_I to derive a distance modulus. Note however that, independent of reddening and distance modulus, the models do predict the correct location of the observed 1H sequence *relative* to the F sequence, for both SMC and LMC.

We also note that the models yield a difference of distance moduli between SMC and LMC of ~ 0.45 , in good agreement with previous determinations based on Cepheids (Laney & Stobie 1994; Udalski et al. 1999c), RR Lyr or Red Clump stars (cf. Udalski et al. 1999c; Udalski 2000). Finally, Caputo et al. (2000) also derived theoretical $\log P - W_I$ relationships for the fundamental mode which are shallower than the present relationships. Alibert et al. (1999) already mentioned and discussed this difference for fundamental mode period – magnitude relationships. As illustrated in Figs. 4 and 5, the Caputo et al. (2000) $\log P - W_I$ relationships are also shallower

compared to the observed data in both SMC and LMC. For the distance moduli adopted in the insets of Figs. 4 and 5, the F sequence of Caputo et al. (2000) reproduce the F data at long period, but merges into the observed 1H pulsators at shorter periods. A variation of the distance modulus cannot clearly solve such discrepancy. This highlights the constraint on models and distance moduli provided by the combination of F and 1H observed sequences.

4. Uncertainties on distance determination

Alibert et al. (1999) analysed the effects of uncertainties inherent to stellar evolution models: convection treatment, overshooting, mass loss, initial helium abundance, etc. The main conclusion is that such uncertainties barely affect the PL relationships and the conclusion on metallicity effects. We however recall that such uncertainties can affect the comparison between models and observations if the *mass* is used as another constraint.

The main uncertainty in our calculations is due to the neglect of convection – pulsation coupling in our linear stability analysis. Convection is frozen in, which means that the perturbation δF_{conv} of the convective flux is neglected in the linearized energy equation. An arbitrary criterion is used to define a red edge for the instability strip (see Alibert et al. 1999 for details), since such approximation cannot yield naturally a red edge.

A time dependent non local theory of convection is required to take into account the effect of convection on pulsation. Such a theory is lacking and the current recipes include several free parameters (cf. Yecko et al. 1998 and references therein). Despite the lack of a robust theory, it has now become clear that convective energy transport is essential to describe the observed properties of pulsating stars such as light curves or Fourier coefficients (Yecko et al. 1998; Feuchtinger 1999; Feuchtinger et al. 2000).

In a systematic analysis based on linear stability analysis of Cepheid models, Yecko et al. (1998) have shown the high sensitivity of the position of the IS to these free parameters, which need to be calibrated according to astronomical observations. But as emphasized by Feuchtinger et al. (2000), even a correct description of the instability strip requires hydrodynamical calculations, since the red edge is determined by nonlinear effects. Even for the blue edge, Feuchtinger et al. (2000) report a shift toward higher T_{eff} by about 350 K for the fundamental mode when convection is included in the pulsation calculation.

In the present paper, we derive a rough estimate of the sensitivity of the period – magnitude relationships derived under the afore-mentioned approximations, and the effects on distance determination. A more detailed analysis and the quantification of uncertainties resulting from convection will be addressed in a forthcoming paper (Alibert & Baraffe 2001). Since our results yield a general good agreement with the width of observed instability strips (see Alibert et al. 1999), a first estimate of such uncertainties can easily be derived by shifting arbitrarily both the

blue and red edges of the instability strip toward cooler or hotter T_{eff} , keeping the width unmodified. In the following, we focus on fundamental PL relationships, since they are mostly used for distance determinations. Inspired by the afore-mentioned results by Feuchtinger et al. (2000), we adopt a shift in T_{eff} of 350 K. Based on the models appropriate for the LMC ($Z = 0.01$), a shift by 350 K toward hotter (cooler) T_{eff} yields brighter (fainter) magnitudes at a given P . The effect decreases toward near-IR filters: the resulting variation of the magnitude in the B -band reaches up to 0.6 mag, it does not exceed 0.3 mag in the I -band and remains below 0.2 mag at longer wavelengths. This is expected, given the decreasing sensitivity to T_{eff} of the flux toward longer wavelengths. In the V -band, M_V varies from 0.3 mag at short P ($\log P = 0.5$) up to 0.45 mag at longer P ($\log P = 1.7$). In the K band, the effect is less than 0.1 mag on the whole range of periods. This simple test highlights the high sensitivity of distance determinations based on theoretical $P - M_V$ relationships, since a variation of 350 K on the location of the blue or red edge can easily result from uncertainties due to convection (see Yecko et al. 1999; Feuchtinger et al. 2000; Alibert & Baraffe 2001).

Finally, since our simple test clearly shows that near-IR period – magnitude relationships are more reliable, it is worth deriving a distance modulus for LMC based on near-IR data. Recent observations in the near-IR (Madore 2000, priv. comm.; Persson et al. 2000) complete data already available from Laney & Stobie (1994) and Gieren et al. (1998). The $P - M_K$ relationship (Table 2) yields a distance modulus for LMC of 18.60–18.70, as illustrated in Fig. 6. Interestingly enough, this distance modulus is in good agreement with the value determined in Sect. 3.3 based on W_I and the combination of F and 1H observed sequences.

5. Conclusion

We have derived period – magnitude relationships for 1H pulsators in different filters. In contrast to fundamental mode, we find a small effect of metallicity in PL relationships for first overtone pulsators. This effect is due to the dependence on metallicity of the ratio P_1/P_0 . Our models reproduce the location of both F and 1H observed sequences of OGLE2 in the SMC and the LMC. Using the reddening free index W_I , models and observations are in good agreement for a LMC distance modulus $\mu_0 = 18.65 - 18.70$. We note however an inconsistency since this value yields a significant discrepancy between predictions and data in the V -band. Such inconsistency may illustrate problems in the choice of the extinction coefficients and the reddening, which are important for the comparison between models and data in the V -band but not crucial for W_I .

We show that an arbitrary shift of 350 K in T_{eff} of the location of the instability strip yields up to 0.45 mag effect on M_V at a given P . Toward near-infrared wavelengths, the effect is smaller and less than 0.1 mag in

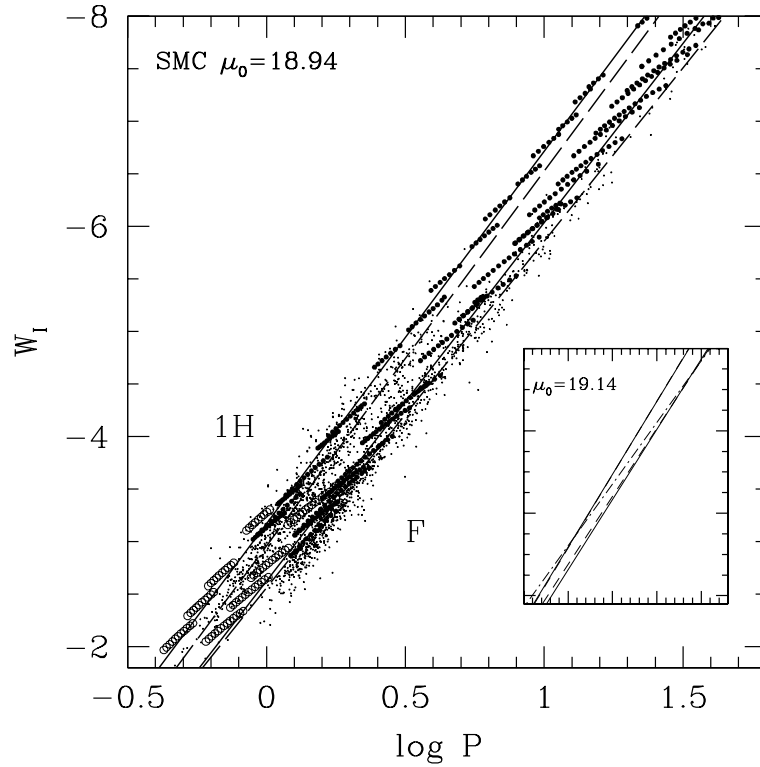


Fig. 4. $\log P$ (in days) – W_I diagram for F and 1H pulsators for models with $Z = 0.004$ and SMC observed Cepheids. Symbols and curves are the same as in Fig. 2. The inset displays only the mean relationships with the same linestyle as in the main figure for a distance modulus $\mu_0 = 19.14$. The dash-dotted curve corresponds to the F relationship of Caputo et al. (2000). Note that for 1H, the theoretical and observed mean relationships are indistinguishable in the inset

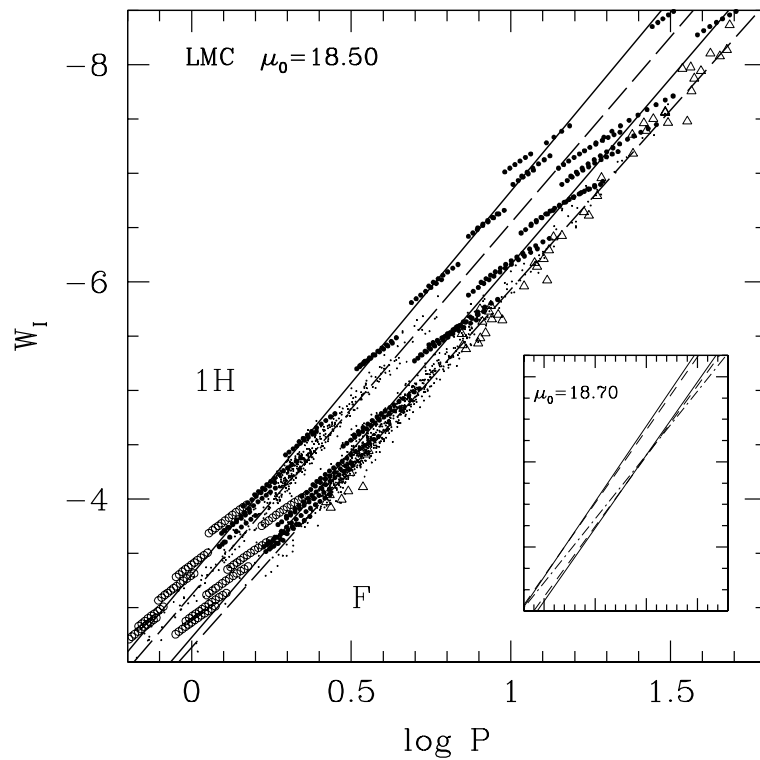


Fig. 5. $\log P$ (in days) – W_I diagram for F and 1H pulsators for models with $Z = 0.01$ and LMC observed Cepheids. Symbols and curves are the same as in Fig. 3. The triangles are observations from Gieren et al. (1998). The inset displays only the mean relationships with the same linestyle as in the main figure for a distance modulus $\mu_0 = 18.70$. The dash-dotted curve corresponds to the F relationship of Caputo et al. (2000)

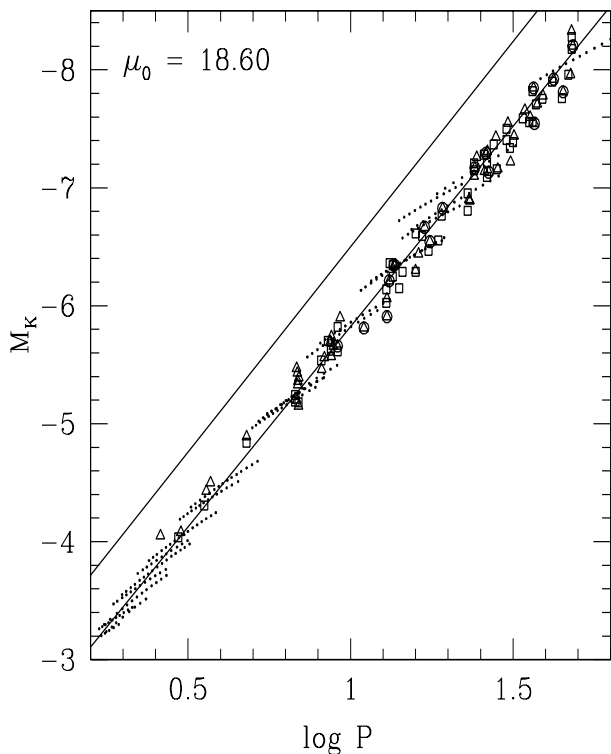


Fig. 6. $\log P$ (in days) – M_K diagram for LMC observed Cepheids. The dots correspond to models for fundamental mode pulsators during core He burning, with $Z = 0.01$. The open squares are from Persson et al. (2000). The triangles are observations from Gieren et al. (1998). The open circles are from Laney & Stobie (1994). The 2 solid curves are the theoretical mean PL relationships for respectively F (lower curve) and 1H (upper curve)

the K -band. Using recent Cepheid data in *the K-band for fundamental pulsators* in the LMC, the models predict a distance modulus for LMC $\mu_0 = 18.60 - 18.70$, in good agreement with the predictions based on W_I and *combined 1H and F data*.

Although Cepheid observations in the V -band are widely used for distance determination, we stress the high uncertainties inherent to observations in this filter (reddening correction, intrinsic dispersion in the instability strip, etc.) and the high sensitivity of $P - M_V$ relationships to theoretical uncertainties. We also emphasize that even if the coupling between convection and pulsation provides a large source of uncertainty in the present work and in all current theoretical calculations, predictions in the K -band are expected to be much less affected by such uncertainty.

Acknowledgements. We are indebted to Andrzej Udalski for providing data and results prior to publication. We are grateful to Barry Madore for valuable discussions and for making available to us near-IR data for the LMC. Many thanks to our referee, A. Gaultschi, who contributed to the improvement of the manuscript and provided excellent ideas. The calculations were performed using facilities at Centre d'Études Nucléaires de Grenoble.

References

- Afonso, C., et al. (EROS) 2000, A&AS, submitted [[astro-ph/9907355](#)]
 Alcock, C., et al. (MACHO) 1997, ApJ, 486, 697
 Alibert, Y., Baraffe, I., Hauschildt, P. H., & Allard, F. 1999, A&A, 344, 551
 Alibert, Y., & Baraffe, I. 2001, in preparation
 Baraffe, I., Alibert, Y., Méra, D., Chabrier, G., & Beaulieu, J.-P. 1998, ApJ, 499, L205
 Bauer, F., et al. 1998, A&A, 348, 175
 Bessell, M. S. 1990, PASP, 102, 1181
 Caputo, F., Marconi, M., & Musella, I. 2000, A&A, 354, 610
 Cox, J. P. 1980, Theory of Stellar Pulsations (Princeton University Press), 108
 Epstein, I. 1950, ApJ, 112, 6
 Feuchtinger, M. U. 1999, A&AS, 136, 217
 Feuchtinger, M. U., Buchler, J. R., & Kollath, Z. 2000, ApJ, accepted [[astro-ph/0005230](#)]
 Freedman, W. 2000, David Schramm Memorial Volume of Physics Report [[astro-ph/9909076](#)]
 Gieren, W. P., Fouqué, P., & Gomez, M. 1998, ApJ, 496, 17
 Groenewegen, M. A. T. 2000, A&A, accepted [[astro-ph/0010298](#)]
 Laney, C. D., & Stobie, R. S. 1994, MNRAS, 266, 441 (LS94)
 Leggett, S. K. 1992, ApJS, 82, 351
 Madore, B. F., & Freedman, W. L. 1991, PASP, 103, 933
 Renault, C., et al. 1996, 12th IAP Astr. meeting, Astrophysical returns of microlensing surveys, ed. R. Ferlet, & J. P. Maillard
 Persson, E., et al. 2000, in preparation
 Schlegel, D. J., Finkbeiner, D. P., & Davies, M. 1998, AJ, 500, 525
 Udalski, A. 2000, AcA, 50, 279
 Udalski, A., Kubiak, M., & Szymanski, M. 1997, AcA, 47, 319
 Udalski, A., Soszynski, I., Szymanski, M., et al. 1999a, AcA, 49, 223
 Udalski, A., Soszynski, I., Szymanski, M., et al. 1999b, AcA, 49, 437
 Udalski, A., Szymanski, M., Kubiak, M., et al. 1999c, AcA, 49, 201
 Whitney, C. A. 1983, ApJ, 274, 830
 Yecko, P. A., Kollath, Z., & Buchler, J. R. 1998, A&A, 336, 553